View Article Online
DOI: 10.1039/C7CE00835J

Journal Name

ARTICLE

Order-disorder phase transition induced by proton transfer in a co-crystal of 2,4-dichlorobenzoic Acid and Trimethylamine N-oxide

Received 00th January 20xx,
Accepted 00th January 20xx

DOI: 10.1039/x0xx00000x

www.rsc.org/

R. F. D'Vries,[a]* R. Moreno-Fuquen,[b] I. Camps,[c] A. P. Ayala,[d] A. R. Kennedy,[e] E. W. Reinheimer[f] and J. Ellena.[g]

The crystalline binary adduct between the trimethylamine N-oxide (TMANO) and 2,4-dichlorobenzoic acid (2,4-DCBA) molecules was obtained by slow evaporation from acetonitrile. The obtained molecular complex is formed by a racemic mixture of molecular complexes crystallizing in the orthorhombic space group Pbca. An exhaustive analysis of the temperature dependence of the cell parameters and the behavior of the acidic hydrogen position and carboxilate group were studied by single crystal and powder X-ray diffraction, FT-IR spectroscopy and theoretical calculations. The molecular system was thermally characterized, subsequently demonstrating a order-disorder transition. Finally, the intermolecular interactions were analyzed via Hirshfeld surface analysis.

Introduction

The design and synthesis of molecular compounds and co-crystals is a novel scientific topic because they are involved in both the biological processes related to molecular recognition as well as chemical self-assembly reactions. Some organic molecular compounds can be used in the design of potential new solid state materials used, for example, in non-linear optics,[1, 2] molecular machines[3, 4] or biological process.[5] The design and synthesis of molecular complexes have also been used to develop new solid forms of active pharmaceutical ingredients[6] and for the analysis of the structural changes associated with different physical or chemical stimuli in supramolecular complexes or polymeric compounds.[7] These stimuli should generate phase transitions or internal molecular motion in the crystal which may give rise to interesting dynamic phenomena.[8, 9] The study of new molecular compounds contributes to the understanding of the formation mechanisms and their applications to crystal engineering and supramolecular chemistry.[10]

As it is well known that different classifications exist for molecular solids depending on the number of components, whether proton transfer occurred and the presence of solvents or inorganic ions in the crystal structure. A co-crystal is a crystalline solid formed by two or more molecular and/or ionic components in the same crystal lattice, while a molecular salt is authored by proton transfer from a donor molecule (acid) to an acceptor molecule (base) as a function of the ionic character of the bond.[11-13]

Our research group has been working for several years on the structural analysis of a variety of molecular compounds,[14, 15] pharmaceutical co-crystals[16-18] and MOFs[19-23] exploring the structure-property correlations in the solid state. In the present work, we report an uncommon case of a molecular complex with an order-disorder conformational transition. This phenomenon refers to the population of disorder conformers as a function of increasing temperature which generates changes in the conformation of the unit cell contents. Using single crystal X-ray diffraction (SCXRD), powder X-ray diffraction (PXRD) and thermal analysis (DSC, TG and HSM), it was for first time related an order-disorder transition phase with a structural disorder around the carboxylate group and the cell expansion. Also, It was theoretically studied the dynamic nature of the O···H···O interaction[24, 25] and it influence in the formation mechanism of the enantiomeric complexes.

[a] Universidad Santiago de Cali, Calle 5 # 62-00, Cali, Colombia.
[b] Departamento de Química - Facultad de Ciencias, Universidad del Valle, Apartado 25360, Santiago de Cali, Colombia.
[c] Laboratório de Modelagem Computacional—LaModel, Instituto de Ciências Exatas, Universidade Federal de Alfenas—Unifal-MG, CEP 37130-000 Alfenas, Minas Gerais, Brazil.
[d] Departamento de Física, Universidade Federal do Ceará, CP 6030, 60440-900, Fortaleza, CE, Brazil.
[e] WestCHEM, Department of Pure and Applied Chemistry, University of Strathclyde, 295 Cathedral Street, Glasgow G1 1XL, Scotland.
[f] Rigaku Oxford Diffraction • 9009 New Trails Drive • The Woodlands, TX 77381 USA
[g] Instituto de Física de São Carlos, Universidade de São Paulo, USP, São Carlos, SP, Brazil.

† Footnotes relating to the title and/or authors should appear here.

Electronic Supplementary Information (ESI) available: [Experimental X-ray powder patterns vs temperature, TG and DSC analysis, IR spectra and crystallographic data and refinement parameters for TMANO-2,4-DCB molecular complex in $P2_12_12_1$ space group]. CCDC reference number 1545106-1545110 contains the supplementary crystallographic data for this paper. This data can be obtained free from the Cambridge Crystallographic Data Centre via: www.ccdc.cam.ac.uk/data_request/cif. See DOI: 10.1039/x0xx00000x

View Article Online
DOI: 10.1039/C7CE00835J

Experimental Section

General information

All reagents and solvents employed were commercially available and were used as supplied without further purification: 2,4-dichlorobenzoic acid and trimethylamine N-oxide (98%, Sigma-Aldrich). IR spectra were recorded from KBr pellets in the 4000-250 cm^{-1} range on a FT-IR nicolet 8700 with Harrick Scientific temperature controller. TGA and DSC analysis were performed in Shimadzu TGA-50 and DSC-60 equipments, respectively, at 25-200 ˚C temperature range using nitrogen (100 mL/min flow) atmosphere and 10 ˚C/min heating rate. Hot-stage microscopy (HSM) was carried out on a Linkam T95-PE device coupled to a Leica DM2500P optical microscope.

Synthesis

The TMANO-2,4-DCB molecular complex was obtained by addition of 2,4-dichlorobenzoic acid (0.128 g, 0.665 mmol) into a solution of TMANO (0.05 g, 0.665 mmol) in acetonitrile (6 ml) under constant stirring at room temperature for 15 minutes. The reaction mixture was slowly evaporated in a desiccator at room temperature. Long prismatic colourless crystals were obtained after 15 days.

Single-Crystal structure determination

Single-crystal X-ray data for TMANO-2,4-DCB molecular complex were collected at different temperatures (100, 150, 200, 250, 298 K) on a Rigaku Oxford Diffraction SuperNova AS2 diffractometer using CuKα radiation (1.54184). Data reduction was carried out using CrysAlis^{Pro}.[26] The structure was solved by SHELXS-2014 software, and then refined by SHELXL-2014,[27, 28] included in WinGX[29] and Olex2.[30] Non-hydrogen atoms of the molecules were clearly resolved and their full-matrix least-squares refinement with anisotropic thermal parameters was conducted. Aromatic and methyl hydrogen atoms were stereochemically positioned and refined with the riding model (with Uiso(H) = 1.2Ueq).[27] The electron density of the hydrogen atom associated with the hydrogen interaction (H1) was located from the Fourier difference maps and its position was refined isotropically. The anisotropic displacement ellipsoid plots were prepared with Diamond,[31] TOPOS[32] and Mercury[33] software packages.

Computational Details

The calculations of the crystal energies were performed using the density functional theory (DFT) methodology for periodic systems.[34, 35] Those DFT calculations were implemented using SIESTA code.[36]

RESULTS AND DISCUSSION

Structural description

Anisotropic displacement ellipsoid plots for the molecular complexes and their corresponding atomic numbering schemes are shown in Figure 1. Details of data collection, refinement and crystallographic data for TMANO-2,4-DCB molecular complex at different temperatures are summarized in Table 1.

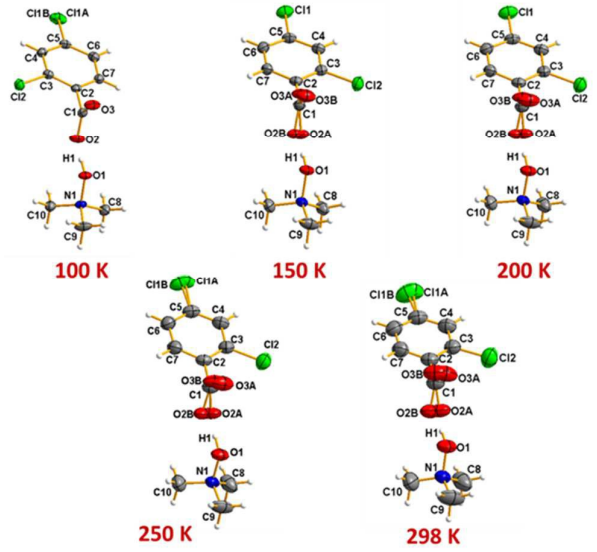

Figure 1. Anisotropic displacement ellipsoid plots at 50% probability for the TMANO-2,4-DCB molecular complex at different temperatures.

View Article Online
DOI: 10.1039/C7CE00835J

Table 1. Crystallographic data and refinement parameters for TMANO-2,4-DCB molecular complex at different temperatures.

	1	2	3	4	5
Emp. Formula	$C_7H_4O_2Cl_2{\cdot}C_3H_9NO$				
FW (g/mol)	266.11	266.11	266.11	266.11	266.11
Temp. (K)	100	150	200	250	298
λ (Å)	1.54184				
Crystal system	Orthorhombic				
Space Group	Pbca				
Unit cell					
a (Å)	12.1285(1)	12.16203(8)	12.20172(7)	12.2403(1)	12.2769(1)
b (Å)	7.92362(7)	7.94027(6)	7.95904(5)	7.9788(1)	8.0018(1)
c (Å)	25.8171(2)	25.8738(2)	25.9260(1)	25.9695(2)	26.0006(2)
Volume ($Å^3$)	2481.07(3)	2498.62(3)	2517.77(3)	2536.26(4)	2554.23(4)
Z	4				
ρ calcd (mg/m^3)	1.425	1.415	1.404	1.394	1.385
Abs.Coeff (mm^{-1})	4.667	4.634	4.599	4.565	4.534
F(000)	1104	1104	1104	1104	1104
θ range (°)	4.0 to 74.1	3.4 to 74.0	3.4 to 74.1	3.4 to 74.0	3.4 to 74.1
Refl. collected / Unique [R(int)]	47327/4994 [0.037]	47880/5043 [0.034]	48314/5087 [0.031]	48804/5124 [0.029]	48303/5161 [0.034]
Completeness (%)	99.6	99.9	99.9	99.9	99.9
Data / restraints / parameters	2505/0/152	2527/0/171	2550/0/171	2564/0/180	2586/0/180
Gof on F^2	1.09	1.09	1.09	1.08	1.07
R1 [I>2σ(I)]	0.0269	0.0286	0.0324	0.0341	0.0393
wR2[I>2σ(I)]	0.0695	0.0778	0.0876	0.0926	0.1126

The crystalline structures for the TMANO-2,4-DCB molecular complex were determined by single crystal X-ray diffraction at different temperatures. The treatment of the diffraction data showed an orthorhombic system and a symmetry corresponding to the space group Pbca, with one molecule per asymmetric unit. A complementary analysis of the data allowed us to observe the presence of two molecules in the asymmetric unit (Figure 2) and solve the structure in a Pseudo $P2_12_12_1$ space group.In this last condition, similar R1 values and flack parameters close to 0.5 were found (see Supp. Inf. S1).

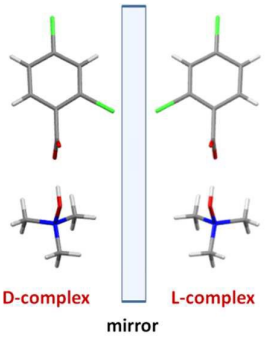

Figure 2. Representation of the two enantiomeric complexes.

The observed electron density for H1 in the 100 - 298 K temperature range is positioned along the O···O segment. The tendency to share or shift the acidic hydrogen to the N-oxide group generates the molecular salt.[37, 38] These results are in agreement with those presented for the urotropine N-oxide and formic acid complex where the electron density concentration associated with the strong O···H interaction is centered ~1.16 Å from the formate moiety.[39]

The presence of two enantiomeric molecular compounds in the crystal seems to be the result of a two-step formation mechanism (Scheme 1) that involves the transference of the acidic proton to the N-oxide molecule in the first step. This step is subsequently followed by the formation of the hydrogen interaction in the crystallization process (Scheme 1). Table 2 shows the distances involved in the hydrogen bonding interactions, noting the slight positional change of the hydrogen atom when the diffraction temperature is increased. In addition, important changes in the C-O distances and disorder in the carboxylate groups also occurred, suggesting the presence of a dynamic process occurring within the unit cell.

The kinetics of the proton transfer between an acid HA (donor) and a base B (acceptor) also can be explained in terms of the ΔpKa rule proposed by Bhogala *et al.*,[40]. The obtained value of ΔpKa = 1.92 indicates the general tendency to yield a proton and form an ionic co-crystals. Although the pKa values are solvent dependent, the tendency is maintained in acetonitrile and the acid is deprotonated in the initial phase of the crystallization processes (Scheme 1). During crystallization, the 2,4-DCBA anion offers two oxygen atoms capable to form the O···H···O adduct within the enantiomeric forms.

Scheme 1. Formation mechanism for the TMANO-2,4-DCB molecular complex.

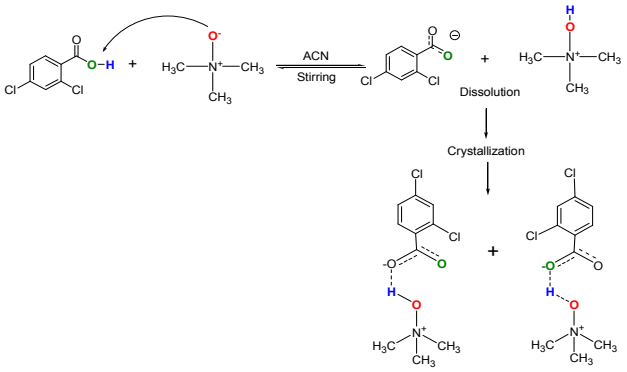

View Article Online
DOI: 10.1039/C7CE00835J

Table 2. Geometric parameters involving the O···H···O interaction at different temperatures.

	D - H	H···A	D...A	D - H···A
Temperature 100 (K)				
O1-H1 ···O2	1.036(2)	1.483(2)	2.519(2)	176.8(2)
Bonds				
N1-O1		1.420(2)		
C1-O2		1.267(2)		
C1-O3		1.233(2)		
Temperature 150 (K)	**D - H**	**H···A**	**D···A**	**D - H···A**
O1-H1 ···O2A	1.016(2)	1.516(3)	2.530(2)	174.4(2)
O1-H2 ···O2B	1.016(2)	1.496(3)	2.507(2)	173.0(2)
Bonds				
N1-O1		1.418(2)		
C1-O2A		1.291(2)		
C1-O2B		1.253(2)		
C1-O3A		1.245(2)		
C1-O3B		1.216(2)		
Temperature 200 (K)	**D - H**	**H ···A**	**D···A**	**D - H···A**
O1-H1 ···O2A	1.042(3)	1.482(3)	2.518(2)	172.2(3)
O1-H1···O2B	1.042(3)	1.471(3)	2.509(2)	172.7(3)
Bonds				
N1-O1		1.417(2)		
C1-O2A		1.265(3)		
C1-O2B		1.277(2)		
C1-O3A		1.238(2)		
C1-O3B		1.220(2)		
Temperature 250 (K)	**D - H**	**H···A**	**D···A**	**D - H···A**
O1-H1 ···O2A	1.049(3)	1.466(4)	2.512(1)	174.3(3)
O1-H1···O2B		1.476(3)	2.513(1)	168.6(3)
Bonds				
N1-O1		1.417(2)		
C1-O2A		1.266(2)		
C1-O2B		1.269(2)		
C1-O3A		1.241(2)		
C1-O3B		1.207(2)		
Temperature 298 (K)	**D - H**	**H ···A**	**D···A**	**D - H···A**
O1-H1 ···O2A	1.012(3)	1.507(4)	2.512(1)	171.3(3)
O1-H1···O2B		1.506(4)	2.511(1)	171.5(3)
Bonds				
N1-O1		1.414(2)		
C1-O2A		1.261(1)		
C1-O2B		1.273(2)		
C1-O3A		1.208(2)		
C1-O3B		1.243(2)		

The conformational variations occurring within the unit cell are due to a dependence on the temperature and lead to an increase in the unit cell parameters when the temperature increases. As demonstrated in Figure 3, it is possible to observe a 2.86% increase in the cell volume as well as 1.21%, 0.98% and 0.71% incremental increases in the unit cell parameters a, b and c respectively. Linear thermal expansion coefficients were calculated from the single crystal diffraction experiment in the 100-298 K range (see Supp. Inf. S7).[41] Values of 62, 50.1 and 36 MK^{-1} were obtained for the crystallographic axes [100], [010] and [001] respectively, while 150 MK^{-1} was obtained for the volumetric coefficient. These values, represent the first time that anisotropic thermal expansion values have been reported for an ionic co-crystal, albeit slightly lower than those reported for co-crystals or organic materials.[8, 42, 43]

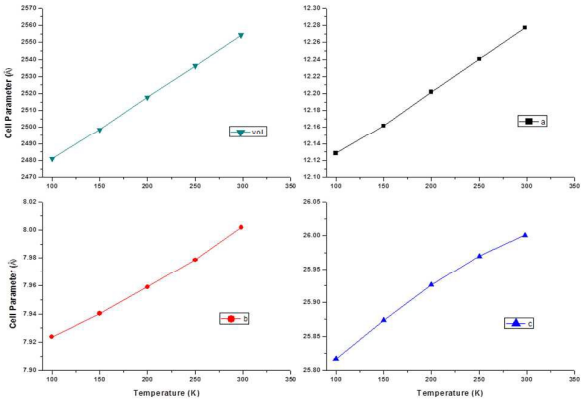

Figure 3. Effect of the temperature on structural parameters.

In order to observe the behavior to temperatures higher than 298 K, variable temperature X-ray powder diffraction analyses were performed. During heating, the peaks are shifted to lower angles, ultimately returning to their original values during cooling and demonstrating the expansion-contraction process of the cell (Figure 4). The changes in the unit cell parameters (see Supp. Inf. S2), associated to the structural dynamic and its direct influence with temperature changes, indicates a concerted and collective motion equilibrium by order-disorder transitions in the crystal.[9]

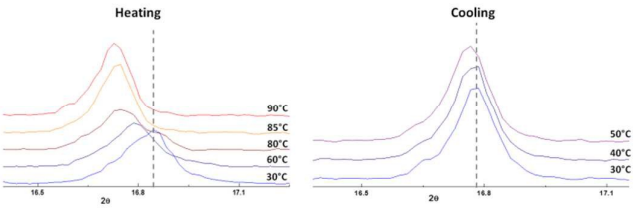

Figure 4. Changes in the [113] peak position within the TMANO-2,4-DCB x-ray powder diffraction pattern during heating and cooling.

Theoretical analysis.

In molecular crystals, as well as in co-crystals, the main cohesive intermolecular interactions are dispersion forces, dipole-dipole forces and hydrogen bonds. In solid-state simulations, the most used approximations in DFT calculations are the local density approximation (LDA) and the generalized gradient approximation (GGA). However, both approximations fail to predict geometric parameters and intermolecular interactions when applied to molecular crystals. In recent work, a new approximation named the van der Waals density functional (vdW-DF) has been developed to overcome these deficiencies.[44-49] In the present work, we used a high-accuracy second version of the van der Waals functional (vdW-DF2) as proposed by Lee *et al.*[49]. To avoid the explicit treatment of the

View Article Online
DOI: 10.1039/C7CE00835J

core electrons, norm conserving Troullier–Martins pseudopotentials[50] were generated with the ATOM software (part of the SIESTA package). For the valence electrons, we used a split-valence double-zeta basis set with polarization functions (DZP).[51] To obtain sufficiently accurate results, convergence studies were done for the mesh cutoff energy. The total energy convergence for the systems was obtained for a mesh cutoff of 300 Ry; however, in our present analyses 350 Ry was used to ensure accuracy. The structure optimizations were done until the Hellman-Feynman forces were below 0.01 eVÅ^{-1} and the energy convergence criterion equaled 10^{-6}.

To understand the effect of the H1 proton position along the O1···O2 segment, a systematic study of the crystal energy was carried out as a function of the H1-O2 distance (Figure 5). To accomplish this, starting from the experimental CIF file[52] and using a Linux batch script, several new CIF files were generated. Then, using the software CIF2Cell,[53] the SIESTA input files were obtained. Through analysis of the effect of the H1 proton position along the O1···O2 segment on the energy, it is possible to observe a minimum between 1.3014 and 1.4557 Å (Figure 5). Such a plot demonstrates the enhanced propensity for proton transfer from the 2,4-DCBA within the new TMANO-2,4-DCBA system in agreement with the single crystal X-ray data (Table 2).

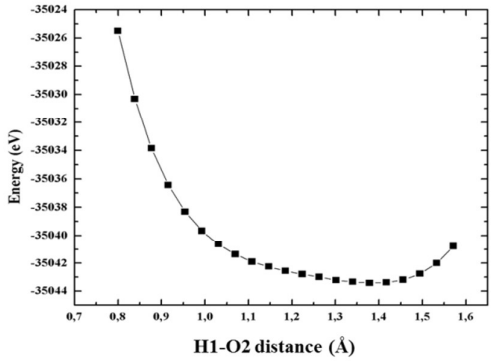

Figure 5. Calculated energy vs. H1-O2 distance in the O1···O2 segment.

Supramolecular Analysis

A Hirshfeld surface analysis was proposed to discern the intermolecular interactions. The color pattern on the d_{norm} surface highlights contacts shorter than the sum of the van der Waals radii in red. Contacts close to their van der Waals limits are colored white, while blue represents longer contacts.[54, 55] This analysis showed that the molecular compound contained shorter O···H and H···O interactions, which represent 13.5 and 12.0 % of the surface, respectively. The Cl···H-C and C-H···Cl contacts combined represent the 29.8% of that surface. The interactions involving the aryl and methyl hydrogen atoms (H···H interactions) represent 25.8% of the surface and are depicted in Figure 6b in blue. The enantiomeric forms obtained in this work present quite similar fingerprinting patterns[56] (Figure 6, c).

The supramolecular studies agree with the Hirshfeld analysis, within which were found C-H···O interactions with distances around 2.483 and 2.678 Å between the methyl groups of the TMANO and the oxygen of the carboxylic acid. In addition, Cl···H-C interactions were observed with distances ranging between 2.906 and 3.150 Å. Ultimately, the 3D supramolecular structure within TMANO-2,4-DCB is formed by the stacking along the [010] direction of R or L pairs in an A···B···A···B type arrangement (Figure 7).

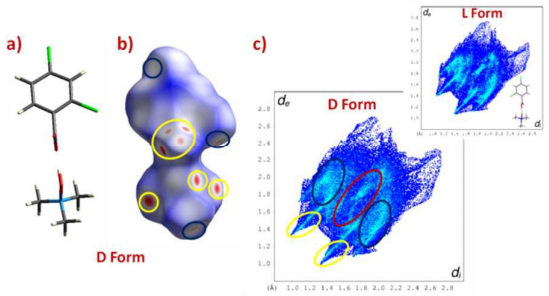

Figure 6. a) Molecular representation in the same orientation of b) d_{norm} Hirshfeld surface (circled in Yellow: O···H and H···O interactions, in Blue: Cl···H and H···Cl interactions and Red: H···H interactions). c) Bidimensional fingerprint plot for whole Form A complex (Calculated with: CrystalExplorer).[57]

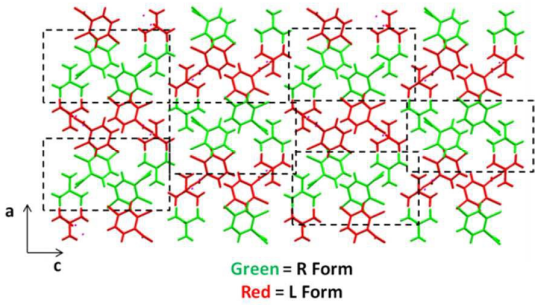

Figure 7. Crystal packing view along [010] direction showing in green and red the R and L pairs, respectively.

Thermal Analysis

The thermal profile for the TMANO-2,4-DCB molecular complex was obtained combining different techniques such as TG, DSC and HSM, in combination with FT-IR vs T and PDRX vs T. DSC analysis demonstrated two characteristic endothermic peaks with onset temperature around 63 and 120 °C. The peak at high temperature is attributed to a melting process followed by decomposition as observed by the TG and HSM analyses (Supp. Inf. S5). The low temperature peak (63°C) is attributed to an order-disorder transition process that is responsible for transforming Phase 1 into a second phase (Phase 2). Once cooled, the sample undergoes a second order-disorder transition to obtain a third phase (Phase 3). In the second and third cycles, the molecular complex undergoes two phase transitions during heating at ~56 and 63°C, ultimately returning to the most stable (Phase 3) during cooling (around 45°C). This behavior suggests that the order-disorder phase transition is a hysteretic process when going through the first

View Article Online
DOI: 10.1039/C7CE00835J

transition to obtain the most stable phase (Phase 3) (see Figure 8). In fact, this can be clearly observed in the values of cell parameters *a* and *b,* obtained by Reitveld refinement of the PXRD patterns (Supp. Inf. S2), where after two heating-cooling cycles the values change when return to room temperature. In summation, these studies demonstrate that the high degrees of freedom associated the atoms involved within the hydrogen bond interaction and the structural disorder are responsible for the complex processes associated with the order-disorder phase transition (Figure 8).

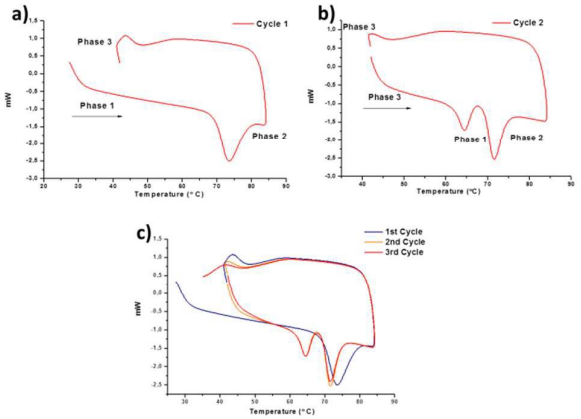

Figure 8. DSC analysis a) first cycle, b) second cycle and c) three complete cycles of heating-coling for the TMANO-2,4-DCB molecular complex.

FT-IR analysis

FT-IR spectra were experimentally measured for TMANO-2,4-DCB molecular complex at the different temperatures, yielding analogous IR profiles in all cases (see Supp. Inf.). Vibrational bands were assigned as follows: The C-H aromatic and aliphatic vibrations are assigned to the bands around ~3040-2725 cm^{-1} in all the cases. The band associated with the O-H vibration is clearly present in 3400 cm^{-1}. Vibrational bands for the asymmetric C=O vibration and C-O vibration of the carboxylate group were present around ~1700 and 1330cm^{-1} respectively, with the former demonstrating a loss of intensity as a function of increasing temperature. Finally the band associated with the N-O vibration is present at ~960 cm^{-1} (Supp. Inf. S6). A vibrational analysis as a function of the temperature was performed; however, due to the small structural changes associated with the transitions, no significant changes were observed in the FT-IR spectra.

Conclusions

A new ionic co-crystal was synthesized from the TMANO and the 2,4-DCB with an interesting structural behavior. This compound shows proton transference from the acid to the TMANO molecule that indicates a two steps crystallization mechanism and the formation of a racemic mixture crystal. This result agrees with reported results that show the tendency for proton transfer to occur in the presence of the N-oxide group. DFT calculations were performed to correlate the H1 atom position in the O1···O2 segment in both the experimental data and in the optimized position are demonstrate the potential to obtain an excellent approximation of the hydrogen atoms positions from experimental medium-to-high resolution X-ray data. A disorder around the carboxylate group with temperature increases generate an order-disorder transition to be clearly observed through DSC and HS microscopy. This transition leads to positive thermal expansion coefficients that were observable by SCXRD and PXRD. It was possible related the structural disorder tendency by temperature increasing observed in the SCXRD and PXRD with the thermal expansion of the cell and order-disorder phase transition observed in the DSC. Hirshfeld surface and 2D finger print plots were used to observe and quantify the interactions present in the crystal packing and indicate that this complex is governed by weak C-H···Cl and Van der Waals interaction, in addition to the O-H···O interaction that give rise to the complex formation.

AUTHOR INFORMATION

Corresponding Author

* To whom correspondence should be addressed. E-Mail: richard.dvries00@usc.edu.co Fax: (+57 2) 518 3000.

Acknowledgements

R.D. Acknowledges to Coordenação de Aperfeiçoamento de Pessoal de Nivel Superior for the CAPES/PNPD scholarship from Brazilian Ministry of Education and the Universidad Santiago de Cali. Thanks to G. Gomez for the FT-IR vs T. I.C. acknowledges the Brazilian agency FAPEMIG for financial support. J.E. thanks CNPq for research fellowships. R.M-F thanks to Universidad del Valle, for partial financial support.

References

1. P. N. Prasad and S. P. Karna, *Int. J. Quantum Chem*, 1994, **52**, 395-410.
2. P. N. Prasad and D. J. Williams, *Nonlinear Optical Effects in Molecules and Polymers*, Wiley, New York, 1991.
3. C. S. Vogelsberg and M. A. Garcia-Garibay, *Chem. Soc. Rev.*, 2012, **41**, 1892-1910.
4. E. L. Romero, R. F. D'vries, F. Zuluaga and M. N. Chaur, *J. Brazilian Chem. Soc.*, 2015, **26**, 1265-1273.
5. E. J. Denning, D. Thirumalai and A. D. MacKerell Jr, *Biophys. Chem.*, 2013, **184**, 8-16.
6. O. Almarsson and M. J. Zaworotko, *Chem. Commun.*, 2004, 17, 1889-1896.
7. W. R. Browne and B. L. Feringa, *Nat Nano*, 2006, **1**, 25-35.
8. K. M. Hutchins, R. H. Groeneman, E. W. Reinheimer, D. C. Swenson and L. R. MacGillivray, *Chem. Sci.*, 2015, **6**, 4717-4722.

View Article Online
DOI: 10.1039/C7CE00835J

9. M. Suzuki, Y. Maeda, M. Akita, H. Teramae and K. Kobayashi, *Cryst. Growth Des.*, 2014, **14**, 6302-6310.
10. K. R. Seddon and M. Zaworotko, *Crystal Engineering The Design and Application of Functional Solids*, Springer Netherlands, Netherland, 1999.
11. A. Lemmerer, S. Govindraju, M. Johnston, X. Motloung and K. L. Savig, *CrystEngComm.*, 2015, **17**, 3591-3595.
12. G. R. Desiraju, *CrystEngComm.*, 2003, **5**, 466-467.
13. S. Aitipamula, R. Banerjee, A. K. Bansal, K. Biradha, M. L. Cheney, A. R. Choudhury, G. R. Desiraju, A. G. Dikundwar, R. Dubey, N. Duggirala, P. P. Ghogale, S. Ghosh, P. K. Goswami, N. R. Goud, R. R. K. R. Jetti, P. Karpinski, P. Kaushik, D. Kumar, V. Kumar, B. Moulton, A. Mukherjee, G. Mukherjee, A. S. Myerson, V. Puri, A. Ramanan, T. Rajamannar, C. M. Reddy, N. Rodriguez-Hornedo, R. D. Rogers, T. N. G. Row, P. Sanphui, N. Shan, G. Shete, A. Singh, C. C. Sun, J. A. Swift, R. Thaimattam, T. S. Thakur, R. Kumar Thaper, S. P. Thomas, S. Tothadi, V. R. Vangala, N. Variankaval, P. Vishweshwar, D. R. Weyna and M. J. Zaworotko, *Cryst. Growth Des.*, 2012, **12**, 2147-2152.
14. R. Moreno-Fuquen, M. T. d. P. Gambardella and J. Valderrama-N, *Acta Cryst.*, 1998, C**54**, 515-517.
15. R. Moreno-Fuquen, G. Hernandez, A. R. Kennedy and C. A. Morrison, *Acta Cryst.*, 2013, C**69**, 665-670.
16. F. T. Martins, F. F. Guimarães, S. B. Honorato, A. P. Ayala and J. Ellena, *J. Pharm. Biomed. Anal.*, 2015, **110**, 76-82.
17. C. C. P. da Silva, R. d. O. Pepino, C. C. de Melo, J. C. Tenorio and J. Ellena, *Cryst. Growth Des.*, 2014, **14**, 4383-4393.
18. J. Ellena, K. de Paula, C. C. de Melo, C. C. P. da Silva, B. P. Bezerra, T. Venâncio and A. P. Ayala, *Cryst. Growth Des.*, 2014, **14**, 5700-5709.
19. R. F. D'Vries, V. A. de la Peña-O'Shea, N. Snejko, M. Iglesias, E. Gutiérrez-Puebla and M. Á. Monge, *Cryst. Growth Des.*, 2012, **12**, 5535-5545.
20. R. F. D'Vries, M. Iglesias, N. Snejko, E. Gutiérrez-Puebla and M. A. Monge, *Inorg. Chem.*, 2012, **51**, 11349-11355.
21. R. F. D'Vries, M. Iglesias, N. Snejko, S. Alvarez-Garcia, E. Gutierrez-Puebla and M. A. Monge, *J. Mater. Chem.*, 2012, **22**, 1191-1198.
22. R. F. D'Vries, S. Alvarez-Garcia, N. Snejko, L. E. Bausa, E. Gutierrez-Puebla, A. de Andres and M. A. Monge, *J. Mater. Chem. C*, 2013, **1**, 6316-6324.
23. R. F. D'Vries, G. E. Gomez, D. F. Lionello, M. C. Fuertes, G. J. A. A. Soler-Illia and J. Ellena, *RSC Adv.*, 2016, **6**, 110171-110181.
24. A. B. Cairns and A. L. Goodwin, *Chem. Soc. Rev.*, 2013, **42**, 4881-4893.
25. M. A. Asghar, Z. Sun, T. Khan, C. Ji, S. Zhang, S. Liu, L. Li, S. Zhao and J. Luo, *Cryst. Growth Des.*, 2016, **16**, 895-899.
26. CrysAlisPro, Agilent (2014). Agilent Technologies Ltd, Yarnton, Oxfordshire, England.
27. G. Sheldrick, *Acta Cryst.*, 2008, *A***64**, 112-122.
28. G. Sheldrick, *Acta Cryst.*, 2015, C**71**, 3-8.
29. L. Farrugia, *J. Appl. Crystallogr.*, 2012, **45**, 849-854.
30. O. V. Dolomanov, L. J. Bourhis, R. J. Gildea, J. A. K. Howard and H. Puschmann, *J. Appl. Crystallogr.*, 2009, **42**, 339-341.
31. K. Brandenburg & H. Putz, *DIAMOND,* (1999). Crystal Impact GbR, Bonn, Germany.
32. V. A. Blatov, A. P. Shevchenko and D. M. Proserpio, *Cryst. Growth Des.*, 2014, **14**, 3576-3586.
33. C. F. Macrae, I. J. Bruno, J. A. Chisholm, P. R. Edgington, P. McCabe, E. Pidcock, L. Rodriguez-Monge, R. Taylor, J. Van De Streek and P. A. Wood, *J. Appl. Crystallogr.*, 2008, **41**, 466-470.
34. J. P. Perdew, A. Ruzsinszky, L. A. Constantin, J. Sun and G. I. Csonka, *J. Chem. Theory Comput.*, 2009, **5**, 902-908.
35. R. M. Martin, *Electronic Structure: Basic Theory and Practical Methods* Cambridge University Press, 2008.
36. J. M. Soler, E. Artacho, J. D. Gale, A. García, J. Junquera, P. Ordejón and D. Sánchez-Portal, *J. Phys.: Condens. Matter*, 2002, **14**, 2745.
37. S. L. Childs, G. P. Stahly and A. Park, *Mol. Pharmaceutics*, 2007, **4**, 323-338.
38. S. Mohamed, D. A. Tocher, M. Vickers, P. G. Karamertzanis and S. L. Price, *Cryst. Growth Des.*, 2009, **9**, 2881-2889.
39. C. L. Nygren, C. C. Wilson and J. F. C. Turner, *J. Phys. Chem. A*, 2005, **109**, 1911-1919.
40. B. R. Bhogala, S. Basavoju and A. Nangia, *CrystEngComm.*, 2005, **7**, 551-562.
41. M. J. Cliffe and A. L. Goodwin, *J. Appl. Crystallogr.*, 2012, **45**, 1321-1329.
42. D. Das, T. Jacobs and L. J. Barbour, *Nat Mater.*, 2010, **9**, 36-39.
43. S. Bhattacharya and B. K. Saha, *Cryst. Growth Des.*, 2013, **13**, 3299-3302.
44. M. Dion, H. Rydberg, E. Schröder, D. C. Langreth and B. I. Lundqvist, *Phys. Rev. Lett.*, 2004, **92**, 246401.
45. G. Román-Pérez and J. M. Soler, *Phys. Rev. Lett.*, 2009, **103**, 096102.
46. K. Jiří, R. B. David and M. Angelos, *J. Phys.: Condens. Matter*, 2010, **22**, 022201.
47. F. D. John and G. Tim, *J. Phys.: Condens. Matter*, 2012, **24**, 073201.
48. C. De-Li, W. A. Al-Saidi and J. K. Johnson, *J. Phys.: Condens. Matter*, 2012, **24**, 424211.
49. K. Lee, É. D. Murray, L. Kong, B. I. Lundqvist and D. C. Langreth, *Phys. Rev. B*, 2010, **82**, 081101.
50. N. Troullier and J. L. Martins, *Phys. Rev. B*, 1991, **43**, 1993-2006.
51. E. Artacho, D. Sánchez-Portal, P. Ordejón, A. García and J. M. Soler, *phys. status solidi (b)*, 1999, **215**, 809-817.
52. I. D. Brown and B. McMahon, *Acta Cryst.*, 2002, B**58**, 317-324.
53. T. Björkman, *Comput. Phys. Commun.*, 2011, **182**, 1183-1186.
54. J. J. McKinnon, M. A. Spackman and A. S. Mitchell, *Acta Cryst.*, 2004, B**60**, 627-668.
55. A. D. Martin, J. Britton, T. L. Easun, A. J. Blake, W. Lewis and M. Schröder, *Cryst. Growth Des.*, 2015, **15**, 1697-1706.
56. M. A. Spackman and J. J. McKinnon, *CrystEngComm.*, 2002, **4**, 378-392.
57. M. J. Turner, J. J. McKinnon, D. Jayatilaka and M. A. Spackman, *CrystEngComm.*, 2011, **13**, 1804-1813.

View Article Online
DOI: 10.1039/C7CE00835J

Graphical Abstract

Order-disorder phase transition induced by proton transfer in a co-crystal of 2,4-dichlorobenzoic Acid and Trimethylamine N- oxide †

R. F. D'Vries,[a]* R. Moreno-Fuquen,[b] I. Camps,[c] A. P. Ayala,[d] A. R. Kennedy,[e] E. W. Reinheimer[f] and J. Ellena.[g]

CrystEngComm. **2017,**

The crystalline binary adduct between the trimethylamine N-oxide and 2,4-dichlorobenzoic acid was obtained. The molecular system was thermally characterized, subsequently demonstrating an order-disorder transition.